Defining Sudden Stratospheric Warmings in Models: Accounting for Biases in Model Climatologies

Junsu Kim[1], Seok-Woo Son[1]*, Edwin Gerber[2], and Hyo-Seok Park[3]

[1]School of Earth and Environmental Sciences, Seoul National University, Seoul, South Korea

[2]Courant Institute of Mathematical Sciences, New York University, New York, NY, U.S.A.

[3]Korea Institute of Geoscience and Mineral Resources, Daejeon, South Korea

June 13, 2016

* Corresponding author: Seok-Woo Son, School of Earth and Environmental Sciences, Seoul National University, 1 Gwanak-ro, Gwanak-gu, Seoul, 151-742, South Korea

Abstract

A sudden stratospheric warming (SSW) is defined by the World Meteorological Organization (WMO) as zonal-mean zonal wind reversal at 10 hPa and 60°N, associated with a reversal of the climatological temperature gradient at this elevation. This wind criteria in particular has been applied to reanalysis data and climate model output during the last few decades. In the present study, it is shown that the application of this definition to models can be affected by model mean biases; i.e., more frequent SSW appear to occur in models with a weaker climatological polar vortex. In order to overcome this deficiency, a tendency-based definition, which is not sensitive to the model mean bias, is proposed and applied to the multi-model data sets archived for the Coupled Model Intercomparison Projection phase 5 (CMIP5). In this definition, SSW-like events are defined by sufficiently strong vortex deceleration. This approach removes a linear relationship between the SSW frequency and intensity of climatological polar vortex for both the low-top and high-top CMIP5 models. Instead, the resulting SSW frequency is strongly correlated with wave activity at 100 hPa. The two definitions detect quantitatively different SSW in terms of lower stratospheric wave activity and downward propagation of stratospheric anomalies to the troposphere. However, in both definitions, the high-top models generally exhibit more frequent SSW than the low-top models. Moreover, a hint of more frequent SSW in a warm climate is commonly found.

1. Introduction

A sudden stratospheric warming (SSW) is an abrupt warming event in the polar stratosphere. It occurs mostly in mid-winter and almost exclusively in the Northern Hemisphere. During this event, the polar stratospheric temperature increases by several tens of degrees within a few days and eventually becomes warmer than mid-latitude temperature. At the same time, the prevailing westerly wind slows and shifts to an easterly direction ((Quiroz 1975); (Labitzke 1977); (Andrews et al. 1987)). Based on these observations, SSWs has been often defined as a zonal-mean zonal wind reversal in the polar stratosphere. In particular, the onset of SSW is defined as the time at which the 10-hPa zonal-mean zonal wind at 60°N changes its direction from westerly to easterly during the winter (e.g., (Charlton and Polvani 2007)). This simple definition, related to that of the World Meteorological Organization (WMO), which also requires a reversal of the temperature gradient over the polar cap, effectively detects the observed characteristics of SSW ((Palmeiro et al. 2015); (Butler et al. 2015)). As Butler et al. (2015) show that the temperature gradient criterion only affects a very small number of SSWs, we will use the simpler, wind only definition from now when referring to the WMO criterion.

It is important to note that the WMO definition is not the only definition of extreme variability of the stratosphere. As summarized in Palmeiro et al. ((2015)) and Butler et al. ((2015)), many definitions for SSWs appear in the literature. These include an area-integrated zonal wind reversal, a tendency-based definition, a Northern Annular Mode (NAM)-based definition, an Empirical Orthogonal Function (EOF)-based definition, and a two-dimensional vortex moment analysis. Palmeiro et al. ((2015)) documented that the observed frequency of SSW and the associated downward coupling are not highly sensitive to the details of the definitions, although interannual to decadal variability of SSW is somewhat sensitive (particularly the drought of SSWs in the 1990s, cf. Butler et al., (2015)). This indicates that long-term statistics of SSW are not highly sensitive to the definition of SSW. However, this is not necessarily true for climate models in which the climatology and temporal variability differ from observations.

Although application of the WMO definition to the climate model output is straightforward, interpretation of the results is not necessarily obvious. For example, SSWs may occur more frequently in a model if it exhibits larger variability of the polar vortex, or if the climatological polar vortex is weak in the model. In the latter case a case, relatively weak deceleration without strong wave driving can result in wind reversal. As an example, Fig. 1 shows zonal-mean zonal wind at 10 hPa and 60°N during winter 1994–1995 from the reanalysis data and the Coupled Model Intercomparison Project phase 5 (CMIP5) model. The reanalysis data show rapid deceleration of the zonal wind from mid-January to early February (Fig. 1a). However, the westerly does not shift to an easterly, and according to the WMO definition, this case is defined as a minor warming event rather than SSW. In the model, the polar vortex is significantly weaker than observation (Fig. 1b). Under this weak background wind, relatively weak temporal variability can easily lead to wind reversal. Thus, the model exhibits three SSW events between November and March, although the deceleration of the polar vortex is not as pronounced as the minor warming event in the reanalysis data (Fig. 1a). It is thus not obvious how a model is biased if it does not capture the correct frequency of SSWs, and worse, a model could potentially get the correct frequency for the wrong reason, a combination of a weak vortex and weak variability, or vice versa.

[Fig. 1 about here]

This result motivated us to explore the sensitivity of SSW to the model mean bias. For multi-model analysis, previous studies have typically used a WMO-like definition ((Charlton et al. 2007); (Butchart et al. 2011); (Charlton-Perez et al. 2008), (2013)). Because SSW frequency in the model, evaluated by the WMO definition, may be influenced by the model mean bias, it is questionable whether the quantitative assessment of SSW frequency in the literature is robust. Although not explored in detail, Butchart et al. ((2011)) do in fact attributed a large intermodel spread in SSW frequency in their multi-model analysis to the different intensities of the polar vortex.

By considering model mean bias, this work revisits the stratospheric variability and SSW frequency in the state-of-the-art climate models. Following previous studies (e.g., (Charlton-Perez et al. 2013); (Manzini et al. 2014)), the models are roughly characterized by grouping them into high-top and low-top models. The low-top models, which have a comparatively poor representation of stratospheric processes, typically underestimate the observed SSW frequency ((Charlton-Perez et al. 2013)). In this study, it is shown that low-top models underestimate SSW frequency even if a different SSW definition is applied. However, the difference in SSW frequency between the high-top and low-top models becomes smaller when the model mean bias is considered.

This paper is organized as follows. In sections 2 and 3, the data used in this study and the definition of SSW are described. Section 4 explores the climatology, interannual variability, and SSW frequency in the historical simulations. In section 5, the results are briefly compared with scenario integrations in order to examine the potential changes in SSW frequency in a warmer climate.

2. Data

The daily-mean zonal-mean zonal wind and geopotential height fields were obtained from the 40-year European Centre for Medium-Range Weather Forecasts (ECMWF) Re-Analysis (ERA40; (Uppala et al. 2005)) for 45 winters of 1957–2002. The results were compared with the state-of-the-art climate models archived for CMIP5 (Table 1). All models that provide both the historical and Representative Concentration Pathway 8.5 (RCP8.5) simulations were used. Most analyses were performed for the historical runs, whereas the RCP8.5 runs were examined to evaluate possible changes in SSW frequency in a warm climate. The analysis period of RCP8.5 runs was set to 45 winters from 2044 to 2099. When multiple ensemble members were available, only the first ensemble member (r1i1p1) was used. An exception is CCSM4, for which the sixth ensemble member (r6i1p1) was used owing to incomplete data in the first ensemble member.

To highlight the model mean bias in the stratosphere, the CMIP5 models were grouped into two subgroups by considering the model top ((Charlton-Perez et al. 2013); (Manzini et al. 2014)). Specifically, models with tops of 1 hPa or higher were classified as high-top models; those with model tops below 1 hPa were classified as low-top models. As described in Table 1, CanESM2 has a model top near 0.5 hPa.

It is ambiguous to place this model into either the high-top or low-top category. Following Manzini et al. ((2014)), this model was therefore classified as a mid-top model.

[Table 1 about here]

It is well documented that after an SSW, stratospheric anomalies tend to propagate downward to the troposphere and the surface. Such downward coupling is often evaluated with a so-called "dripping paint" composite of the NAM index ((Baldwin and Dunkerton 2001)). In this study, rather than using the EOF-based NAM index, however, a simple NAM index was used. The NAM index is computed by integrating the geopotential height anomalies from 60°N to the pole at each pressure level ((Cohen et al. 2002); (Baldwin and Thompson 2009)). The sign is then flipped to obtain a consistent sign convention of the EOF-based NAM index. The resulting time series are then normalized by one standard deviation of the NAM index of ERA40. This ensures that the strength of the variability of one standard deviation in the model is the same as that of one standard deviation in the reanalysis datasets. Specifically, the variability in the models is comparable to that in the reanalysis.

3. Definition of SSW

In this study, the two definitions of SSW were adopted. A WMO-like definition, requiring a zonal-mean zonal wind reversal at 10 hPa and 60°N, was used as a reference. When an SSW was detected, no subsequent event is allowed within a 20-day interval, the period determined in considereration of the thermal damping time scale at 10 hPa. This allowed us to avoid a double counting of essentially the same event. Final warming events were removed by adopting the method proposed by Charlton and Polvani ((2007)).

As previously discussed, the WMO wind focused definition can be impacted by model mean bias. To reduce such dependency, a new definition based on the zonal-mean zonal wind tendency (e.g., (Nakagawa and Yamazaki 2006); (Martineau and Son 2013)) was also applied. Specifically, an SSW-like event was identified when the tendency of the zonal-mean zonal wind at 10 hPa and 60°N exceeded -1.1 m s^{-1} day^{-1} over 30 days; that is, a change in vortex strength must exceed -33 m s^{-1} over 30 days. The reference latitude and pressure level used in the present study are identical to those used in the WMO definition to enable direct comparison.

The two free parameters, i.e., the threshold value of deceleration (-1.1 m s^{-1} day^{-1}) and the time window for tendency evaluation (30 days) were determined by referring to the observed SSW. The latter, a 30-day window, was inspired by the correlation analysis of Polvani and Waugh ((2004)). Polvani and Waugh ((2004)) showed that the upward wave activity entering the stratosphere, integrated over 20 days or longer, leads to a marked weakening of the polar vortex. As discussed in section 4, wave activity, which drives SSW, is often maintained for about 30 day; thus, a 30-day window was selected in this study. A slight adjustment of the analysis window (e.g., 20 or 40 days) did not change the overall results, as subsequently described.

The minimum deceleration threshold, -1.1 m s^{-1} day^{-1}, is somewhat arbitrary. In this study, this threshold value was selected simply to recover the WMO wind based SSW frequency. It is known that SSW frequency in the reanalysis data, evaluated at 10 hPa using various definitions, is about 6.4 events per decade ((Butler et al. 2015); (Palmeiro et al. 2015)). The sensitivity of SSW frequency to the threshold value is also discussed subsequently.

It is important to note that the tendency-based definition does not consider a zonal-mean zonal wind reversal. The detected SSW therefore includes major SSW in addition to minor warming events in terms of the WMO definition. As such, the dynamical evolution of SSW in the two definitions is not necessarily the same. Table 2 presents the central dates of SSW events identified by the WMO and tendency-based definitions in ERA40. Only 17 of a total of 29 SSW events, or 60%, were common in the two definitions, which clearly indicates that the detected SSW differed significantly. A major difference appeared in early 1990s. Although no SSW events were identified for 1990 and 1997 in the WMO definition, five SSW events were detected in the tendency-based definition, as clearly shown in Fig. 2. This suggests that while the vortex was abnormally strong over this decade, it was still about as variable as in other decades. Overall, the tendency-based SSW events were more evenly distributed in time. This even distribution, with no significant decadal variability, is somewhat similar to NAM-based SSW, as shown in Fig. 2 of Butler et al. ((2015)).

[Fig. 2 about here]

4. Historical runs

a. Climatology and interannual variability of the polar vortex

Figure 3a shows a vertical cross-section of zonal-mean zonal wind during the Northern Hemisphere winter (December–January–February, DJF) from ERA40. Westerly jets during the boreal winter consist of a tropospheric jet around 30°N and a stratospheric polar vortex around 65°N (Fig. 3a). This structure was effectively captured by the multi-model mean (MMM) of the high-top models (Fig. 3d). The high-top MMM biases are less than 2 m s^{-1} (shaded), which is not significantly different from the ERA40 data over most regions. In contrast, the low-top MMM show a stronger polar vortex than that in the reanalysis data (Fig. 3g). Their mean biases are more than 5 m s^{-1} at 10 hPa and 40°N, indicating that the polar vortex in the low-top models is biased equatorward. Although a causal relationship is unclear, the wind and temperature biases shown in Fig. 3g could partly reflect a lack of SSWs in the low-top models, as compared with reanalyses and the high-top models ((Charlton-Perez et al. 2013)).

[Fig. 3 about here]

The low-top models also exhibit significant biases in their interannual variability. Here, interannual variability is defined by a standard deviation of the DJF-mean zonal-mean zonal wind. The high-top models effectively captured the interannual variability in the extratropical stratosphere (Fig. 3e). The low-top models exhibited significantly larger errors with about 33% less interannual variability than the reanalysis data at 50 hPa and 60°N (Fig. 3h). This result, which agrees well with the findings of Charlton-Perez et al. ((2013)), is to some extent anticipated because the low-top models do not resolve realistic stratospheric processes. It is interesting to note that both high-top and low-top models underestimated tropical stratospheric variability, indicating the failure of simulating quasi-biennial oscillation (QBO; (Kim et al. 2013)). Because the QBO can influence the Northern Hemisphere wintertime stratospheric polar vortex ((Holton and Tan 1980); (Garfinkel et al. 2012)), the lack of QBO activity in the models could adversely affect extratropical stratospheric variability on interannal time scales.

b. Intraseasonal variability of the polar vortex

High-top models are also more realistic than low-top models in terms of their intraseasonal variability (right panels in Fig. 3). The low-top models exhibit larger biases in intraseasonal variability than the high-top models (Figs. 3f, i). These biases are not confined within the stratosphere but extend to the troposphere in high latitudes as well. This could indicate that the poorly represented stratospheric process in the low-top models may introduce bias in the upper troposphere.

The relationship between the deseasonalized daily zonal-mean zonal wind variability and climatological zonal-mean zonal wind at 10 hPa and 60°N is further illustrated in Fig. 4, where the high-top and low-top models reasonably separate into two clusters. The daily variability in the high-top models is about 12 m s^{-1}, which is close to the observation of about 13 m s^{-1}. However, that in the low-top models it is only about 8 m s^{-1}, which possibly indicates less frequent SSWs. In addition, the intermodel spread of the low-top models is larger than that of the high-top models in both climatology and intraseasonal variability. This result confirms those of previous studies such that a high model top is helpful for reproducing the stratospheric mean state and temporal variability ((Charlton-Perez et al. 2013); (Manzini et al. 2014)).

[Fig. 4 about here]

c. SSW statistics

Extending the results of Charlton-Perez et al. ((2013)), the SSW frequency of ERA40 was first evaluated by using the WMO wind definition (Fig. 5a). The long-term mean SSW frequency is 6.4 events per decade, as shown by the horizontal line in the figure. CMIP5 models typically underestimate this frequency ((Charlton-Perez et al. 2013)). The SSW frequency in the high-top models varies from 3 to 9 events per decade (red bars). On average, the frequency was 5.8 events per decade, as shown by the rightmost red bar in the figure, which is reasonably close to the reference frequency. In contrast, the low-top models exhibit only up to 4 events per decade (blue bars in the figure), with 1.8 events per decade on average (rightmost blue bar). This result is significantly smaller than the high-top MMM frequency. More importantly, the intermodel spread in the two groups of models does not overlap, indicating that the low-top models are well separated from the high-top models in terms of SSW frequency, as also shown in Fig. 4. This result supports the findings of Charlton-Perez et al. ((2013)), who analyzed a slightly smaller numbers of CMIP5 models. Somewhat surprisingly, the mid-top model, CanESM2, showed significantly more frequent SSW events than those in other models, with 10.7 events per decade. Such high frequency is associated with a weak background wind in this model, as illustrated in Figs. 1b and 4.

[Fig. 5 about here]

The SSW frequency was also evaluated using the tendency-based definition (Fig. 5b). By construction, the SSW frequency under this definition remains 6.4 events per decade in ERA40. Although each model shows SSW frequencies that differed from the WMO definition, the high-top MMM was 6.2 events per decade, which is quantitatively similar to the observed frequency. Within the uncertainty range, this frequency is also similar to that derived from the WMO definition: the SSW frequency in the

WMO definition is 5.8 events per decade (Fig. 5a), whereas the tendency-based definition illustrates 6.2 events per decades (Fig. 5b). However, the intermodel spread is only half of that of the WMO definition. This suggests that the tendency-based definition is less sensitive to intermodal differences (i.e. biases) as the WMO definition.

The low-top models again exhibited fewer frequent SSW events than the high-top models, with an MMM frequency of 3.7 events per decade. This result indicates that regardless of the definition, the low-top models tend to underestimate the observed SSW frequency. Here, it is important to note that the resulting SSW frequency was larger than that derived from the WMO definition in Fig. 5a, (i.e., 1.8 events per decade), which indicates that the different SSW frequencies between the high-top and low-top models become smaller when a definition free of model mean bias is used. In fact, the intermodel spread of SSW frequency in the low-top models overlaps that in the high-top models, as shown in Fig. 5b. This result indicates that extreme event frequency may be less sensitive to the model top than that previously reported (e.g., (Charlton-Perez et al. 2013)). This is particularly true if the two models with extremely rare SSW events (i.e., CSIRO-Mk3-6-0 and INMCM4) are excluded from the low-top MMM.

The only mid-top model, CanESM2, shows a significant reduction in SSW frequency from the WMO definition to the tendency-based definition, as indicated by the green bars in Figs. 5a and b. When the tendency-based definition is used, the SSW frequency is close to the observed frequency. As noted in section 3, the model classification is based a model top above or below 1 hPa: CanEMS2, in which the model top is 0.5 hPa, was a clear outlier belonging to neither high-top nor low-top models when the WMO definition was used (Fig. 5a). When the tendency-based definition was used, the SSW frequency of this model became similar to that of the high-top models.

Both the WMO wind only and tendency-based definitions utilize zonal-mean zonal wind at a fixed latitude (60°N) to evaluate the polar vortex weakening. This latitude corresponds to the vortex boundary in the reanalysis data ((Butler et al. 2015)). However, the same may not be true when using the models.

In fact, as shown in Fig. 3, the latitudinal structure of polar vortex in the model differs from that in the reanalysis data, and 60°N is not the vortex boundary in all models. This is particularly true for the low-top models (Fig. 3c). To test this possibility, all analyses were repeated by replacing the fixed reference latitude with the model-dependent reference latitudes. The latitude of the maximum zonal-mean zonal wind at 10 hPa in long-term climatology was chosen for each model, and the SSW frequency again evaluated. This modification results in an increased SSW frequency of about half an event per decade in both the high-top and low-top models (not shown). However, the overall conclusion of more frequent SSW in high-top models than those in low-top models does not change.

We also tested the sensitivity of the tendency-based SSW to the threshold value of deceleration and the time window for tendency evaluation. The top panel in Fig. 6 presents the SSW frequency calculated from ERA40 as a reference. As would be expected, the SSW frequency generally increased as the threshold value decreases (i.e., SSW was more frequent for a weaker threshold value). The SSW frequency also decreases with an increase in the time window. Notably, the SSW frequency in the high-top models is comparable to that in ERA40 if the observed SSW frequency of 6–8 events per decade was selected as a reference (near-zero line in Fig. 6c), but would be biased high (low) if stricter (weaker) criteria are applied. The low-top models, however, exhibited a significantly smaller number of SSW events (Fig. 6d) under all conditions. This underestimation is not highly sensitive to the parameters used in the tendency-based SSW definition. Figure 6b further shows the differences in SSW frequency between the high-top and low-top models. In general, the high-top models showed more frequent SSW, which indicates that the SSW frequency difference between the two groups of models is quite robust.

[Fig. 6 about here]

The above results are all based on intercomparison of high-top and low-top models. Individual models, however, are fundamentally different in many aspects such as dynamic core, physics, resolution, and ocean models; therefore, direct comparison of these models may not be straightforward. In this regard, comparison of two different experiments from the same modeling institutes can be useful. As indicated in Table 1, The Centro Euro-Mediterraneo sui Cambiamenti Climatici (CMCC) provides two experiments: that with a climate model (CMCC-CM) and that with a climate model including a stratospheric component (CMCC-CMS). The former is a low-top version, whereas the latter is a high-top version. Figure 5b shows that CMCC-CMS exhibits realistic SSW frequency and significantly more frequent SSW than CMCC-CM, which is consistent with MMM comparison. A pair of experiments from Institut Pierre Simon Laplace Climate model 5A (IPSL-CM5A) including IPSL-CM5A-low resolution (LR) and IPSL-CM5A-medium resolution (MR), which differ in horizontal resolution, further shows that the model with higher horizontal resolution (IPSL-CM5A-MR) has more frequent SSW than IPSL-CM5A-LR. However, MPI-ESM-LR and MPI-ESM-MR, which have different vertical resolutions but the same model top, show a similar SSW frequency. A comparison of the Model for Interdisciplinary Research on Climate-Earth System Model (MIROC-ESM) and that coupled with atmospheric chemistry (MIROC-ESM-CHEM), the latter of which considers interactive chemistry in the stratosphere, also exhibited no significant difference. These results may suggest that SSW frequency is more sensitive to the model top and horizontal resolution than to vertical resolution and interactive chemistry. Additional modeling studies with systematic varying of model configurations are needed to confirm this finding.

To highlight the dependency of SSW frequency to the model mean bias, Fig. 7a illustrates the relationship between DJF-mean zonal-mean zonal wind at 10 hPa and 60°N and SSW frequency derived from the WMO wind definition. The high-top, mid-top, and low-top models are indicated in red, green, and blue, respectively, whereas ERA40 is shown by a black dot. A strong negative correlation was evident with a correlation coefficient of −0.63, which is statistically significant at the 95% confidence level. This clearly indicates that SSW occurred less frequently as the background wind becomes stronger (or, alternatively, fewer SSW leads to a stronger vortex). Such negative correlation was somewhat weak in the low-top models owing to a few outliers that had almost no SSW events. Without these outliers (i.e., CSIRO-MK3-6-0 and MIROC5), the negative correlation is statistically significant.

[Fig. 7 about here]

Figure 7a again shows that the high-top models are well separated from the low-top models. Except for two models, most low-top models exhibited a stronger polar vortex than that by ERA40. This does not allow a wind reversal unless stratospheric wave driving is sufficiently strong (or may inhibit the resonant, vortex splitting mechanism that depends less on the wave driving; Esler and Scott (2005)). This result confirms that the difference between the high-top and low-top models shown in Fig. 5a is caused partly by the model mean biases. Another factor that may explain the less frequent SSW in the low-top models is relative weak wave driving. As shown in Fig. 7c, the low-top models exhibit somewhat weaker wave activity than the high-top models. Here, wave activity was quantified by integrating the zonal-mean eddy heat flux at 100 hPa over 40–70°N.

The right-hand panels of Fig. 7 are identical to those on the left except for the tendency-based definition. The linear relationship, evident in Fig. 7a, essentially disappears (Fig. 7b). Although the low-top models show a statistically significant correlation, the correlation coefficient is positive, which is largely attributed to the two outliers at the bottom left-hand corner. This result suggests that the tendency-based SSW definition is almost independent from any model mean climatological bias. More importantly, the tendency-based definition is strongly correlated with the wave activity at 100 hPa (Fig. 7d) such that more frequent SSW occurs when the wave activity in the lower stratosphere is stronger. This result indicates that the tendency-based definition is more dynamically constrained than the WMO wind based definition. It should be noted that most models tend to underestimate wave activity in the lower stratosphere. This result is consistent with the fact that most models underestimate the SSW frequency regardless of the model top (Fig. 5b).

The relationship among the SSW frequency, daily zonal-mean zonal wind variability, and DJF mean zonal-mean zonal wind at 10 hPa and 60°N is summarized in Fig. 8, which combines the essential results of Fig. 4, 7a, and 7b. The CMIP5 models generally have realistic time-mean polar vortices but too little variability (e.g., climatology of 25–35 m s^{-1} in Fig. 8). Under both the WMO and tendency definitions, they exhibit less frequent SSW with larger intraseasonal variability. The tendency definition clearly exhibits a more linear relationship between the SSW frequency and intraseasonal variability of the polar vortex than that by the WMO definition. Hence changes in SSW frequency can also result in variation of intraseasonal variability in a model.

[Fig. 8 about here]

d. SSW dynamics

The SSW events identified by the two definitions can have different dynamical evolution. For example, linear wave dynamics suggest that vertical propagation of planetary-scale waves, which drive SSW, can be restricted if the zonal wind in the stratosphere becomes easterly. However, this may not be the case in the tendency-based SSW because wind reversal to easterly is not guaranteed. To address this issue, we investigated the wave activity over the course of an SSW. Figure 9 presents a composite of the temporal evolution of a zonal-mean eddy heat flux at 100 hPa integrated over 45–75°N for the two SSW definitions. The heat flux increases before the onset of an SSW, then rapidly decreases afterward. Although the evolution of wave activity is qualitatively similar in the two definitions, the tendency-based definition showed a somewhat slower decay, as shown by the black lines in Fig. 9. This result indicates that some planetary-scale waves propagated into the stratosphere even after SSW, which is consistent with the linear dynamics.

[Fig. 9 about here]

Wind-reversal SSW is associated with slightly stronger and more concentrated wave forcing than that the tendency-based SSW. However, the time-integrated wave activity over 30 days before the onset of SSW is comparable in the two definitions, indicating similar net wave driving. Figure 9 also shows that the wave activity in the high-top models is somewhat stronger than that in the low-top models from lag −20 to 0 days. Consistent with this result, the intensity of SSW events in terms of zonal wind deceleration is somewhat stronger in the high-top models than that in the low-top models (not shown). This result suggests that improved vertical resolution is helpful in simulating more realistic SSWs.

As discussed previously, SSWs have received much attention in recent decades because of its influence on tropospheric circulation and surface climate ((Baldwin and Dunkerton 2001)). By comparing a subset of CMIP5 models, Charlton-Perez et al. ((2013)) reported that high-top models tend to have more persistent anomalies than low-top models in the troposphere. In Fig. 10, a similar comparison is made in terms of NAM-index anomalies for the two SSW definitions. For ERA40, the tendency-based SSW exhibited a stronger phase change than the wind-reversal SSW in the NAM anomalies in both the lower stratosphere and the troposphere (Figs. 10a, b), but an overall weaker (less negative) tropospheric NAM response following the event. Such a difference is also evident in the MMM. These results suggest that the SSWs identified by the two definitions are indeed quantitatively different. However, the overall evolution of SSW and the associated wave driving and downward propagation are qualitatively similar.

[Fig. 10 about here]

It is important to note that SSW-induced NAM-index anomalies in the lower stratosphere tend to persist longer in the high-top models than those in the low-top models (Fig. 10). Similarly, the tropospheric anomalies are stronger and persisted slightly longer in the high-top models than in the low-top models in the two definitions. This result suggests that the timescale of SSW and downward coupling are somewhat sensitive to the model top.

5. SSWS in future climate projections

We now compare the SSW frequency in the recent past with that in the 21st century. Figure 11 illustrates the projected changes in SSW frequency under the RCP8.5 scenario by the end of 21st century. The WMO definition suggests slightly more frequent SSW in the warm climate (Fig. 11a), which agrees well with the results of Charlton-Perez et al. ((2008)). The high-top models generally exhibited a more positive trend in SSW frequency than the low-top models; 8 out of 12 high-top models showed an increasing trend (Fig. 11c). However, the low-top models did not show a clear trend if CSIRO-MK3-6-0, which failed to simulate SSW, was excluded. Half of the low-top models showed increasing and decreasing trends, respectively.

[Fig. 11 about here]

McLandress and Shepherd ((2009)) suggested that the increase in SSW frequency in a warmer climate, as reported by Charlton-Perez et al. ((2008)), may be partly attributed to changes in background wind rather than those in wave activity. By applying a relative definition, they showed that SSW frequency did not change significantly in their model. This idea is evaluated in Fig. 11b with the tendency-based SSW definition. Consistent with the historical simulations, the high-top models capture the observed SSW frequency reasonably well. However, in both groups of models, a weak positive trend in the SSW frequency is observed (Fig. 11b). Although the absolute change is not statistically significant, 21 of 27 CMIP5 models exhibited an increasing trend (Fig. 11d). Such behavior was evident upon separate examination of the high-top and low-top models, with 9 of 12 high-top and 11 of 14 low-top models showing increasing trends. This result may imply that some dynamical properties of SSW, such as planetary wave activity, may change in the future. To identify the dynamical mechanisms, further analyses are needed.

6. Summary and discussion

The present study suggests that the wind metric emphasized by the WMO definition of an SSW -- a wind reversal at 10 hPa and 60°N -- can be impacted by model mean biases ((McLandress and Shepherd 2009)). The definition can straightforwardly be applied to models, but the interpretation may be more complicated. If the climatological polar vortex of the model is stronger than observation, it tends to allow less frequent SSWs. Such a relationship is robustly found in the CMIP5 models, indicating that the previous multi-model studies on wind-reversal SSW are likely influenced by the model mean biases and long-term mean flow changes.

An alternative definition of extreme vortex variability, aimed a making it independent of model mean biases, was proposed in this study. This definition detects SSWs by examining the zonal-mean zonal wind tendency at 10 hPa and 60°N. In this definition, the linear relationship between SSW frequency and the intensity of climatological polar vortex, which is evident in the WMO definition, essentially disappears. More importantly, the SSW frequency becomes highly correlated with wave activity at 100 hPa. This result indicates that the tendency-based definition is more dynamically constrained than the WMO definition.

The tendency-based definition resulted in more frequent SSWs than the WMO definition in the climate models, particularly in the low-top models, even though it was constructed to have no effect on the frequency in ERA-40 reanalysis. This indicates that the significant difference in SSW frequency between the low-top and high-top models reported in previous studies ((Charlton-Perez et al. 2013)) can be attributed, at least partly, to model mean bias rather than wave driving. However, in both definitions, the high-top models exhibited more frequent SSW than the low-top models, consistent with stronger lower-stratospheric wave activities in the high-top models. This result indicates that a high model top and more accurate stratospheric representation are necessary for simulating realistic SSW. It was also found that in both definitions, the SSW frequency tended to increase in a warm climate. These results are qualitatively consistent with those in previous studies (Charlton-Perez et al., (2008), (2013)), although their a quantitative differences. It is important to note that the SSW detected by the different definitions may have different dynamical and physical properties ((Martineau and Son 2015)). In fact, wind-reversal SSW events exhibit evolution that differs quantitatively from the tendency-based SSW. The former is associated with more focused and stronger wave activity than the latter. This difference leads to slightly longer persistence of stratospheric anomalies and a stronger downward coupling in the tendency-based SSW. Such differences need to be considered in comparisons.

It should be emphasized that development of a new SSW definition is not our primary intent in this study. Our objectives were to re-examine the SSW frequency in CMIP5 models by considering the model mean bias and to test the robustness of previous studies by applying the different SSW definitions. Certainly, other approaches can be used to define stratospheric extreme events that are free from model mean biases. Among various SSW definitions ((Butler et al. 2015)), however, the tendency-based definition is likely one of the simplest approaches that can be easily compared with the WMO definition. Because the zonal-mean zonal wind tendency is directly related to divergence in eddy heat flux and momentum flux in the transformed Eulerian mean equation, the tendency-based SSW is closely associated with accumulated wave activity in the stratosphere.

The tendency-based definition has other advantages over the WMO definition with respect to evaluation of models. The tendency-based definition is may be useful for detecting SSW in a changing climate. Previous studies have reported a possible weakening of the polar vortex in response to increasing greenhouse gas concentration (McLandress and Shepherd (2009); Manzini et al. (2014)). Because the background wind becomes weaker, the chances of a wind reversal may increase, resulting in more frequent SSW when the WMO definition is used. Such an increase in SSW frequency, however, could be misleading if the wave forcing does not change systematically (McLandress and Shepherd

2009). Therefore, further discussion on simple, but objective detection of stratospheric extreme events, including vortex weakening events such as SSWs, is important (Butler et al. 2015).

Acknowledgement

The authors thank Dr. Gwangyong Choi for offering helpful comments and discussion. This work was funded by the Korea Meteorological Administration Research and Development Program under Grant KMIPA 2015-2094 and the US National Science Foundation, through grant AGS-1546585.

References

Andrews, D. G., J. R. Holton, and C. B. Leovy, 1987: Middle atmosphere dynamics. Academic Press, 489 pp.

Baldwin, M. P., and T. J. Dunkerton, 2001: Stratospheric harbingers of anomalous weather regimes. Science, 244, 581-584.

Baldwin, M. P., and D. W. J. Thompson, 2009: A critical comparison of stratosphere-troposphere coupling indices. Quart. Jour. Royal. Met. Soc., 135, 1661-1672.

Butchart, N., and Coauthors, 2011: Multimodel climate and variability of the stratosphere. J. Geophys. Res. Atmos., 116, D05102.

Butler, A. H., D. J. Seidel, S. C. Hardiman, N. Butchart, T. Birner, and A. Match, 2015: Defining sudden stratospheric warmings. Bull. Amer. Meteor. Soc., 96, 1913-1928.

Charlton-Perez, A. J., L. M. Polvani, J. Austin, and F. Li, 2008: The frequency and dynamics of stratospheric sudden warmings in the 21st century. J. Geophys. Res., 113, D16116.

Charlton-Perez, A. J., and Coauthors, 2013: On the lack of stratospheric dynamical variability in low-top versions of the CMIP5 models. J. Geophys. Res., 118, 2494-2505.

Charlton, A. J., and L. M. Polvani, 2007: A new look at stratospheric sudden warmings. Part I: Climatology and modeling benchmarks. J. Climate, 20, 449-469.

Charlton, A. J., and Coauthors, 2007: A new look at stratospheric sudden warmings. Part II: Evaluation of numerical model simulations. J. Climate, 20, 470-488.

Cohen, J., D. Salstein, and K. Saito, 2002: A dynamical framework to understand and predict the major Northern Hemisphere mode. Geophys. Res. Lett., 29, 51.

Esler, J. G., and R. K. Scott, 2005: Excitation of Transient Rossby Waves on the Stratospheric Polar Vortex and the Barotropic Sudden Warming. J. Atmos. Sci., 62, 3661-3682.

Garfinkel, C. I., T. A. Shaw, D. L. Hartmann, and D. W. Waugh, 2012: Does the Holton–Tan Mechanism Explain How the Quasi-Biennial Oscillation Modulates the Arctic Polar Vortex? J. Atmos. Sci., 69, 1713-1733.

Holton, J. R., and H.-C. Tan, 1980: The Influence of the Equatorial Quasi-Biennial Oscillation on the Global Circulation at 50 mb. J. Atmos. Sci., 37, 2,220-2208.

Kim, J., K. M. Grise, and S.-W. Son, 2013: Thermal characteristics of the cold-point tropopause region in CMIP5 models. J. Geophys. Res. Atmos., 118, 8827-8841.

Labitzke, K., 1977: Interannual Variability of the Winter Stratosphere in the Northern Hemisphere. Mon. Wea. Rev., 105, 762-770.

Manzini, E., and Coauthors, 2014: Northern winter climate change: Assessment of uncertainty in CMIP5 projections related to stratosphere-troposphere coupling. J. Geophys. Res. Atmos., 119, 2013JD021403.

Martineau, P., and S.-W. Son, 2013: Planetary-scale wave activity as a source of varying tropospheric response to stratospheric sudden warming events: A case study. J. Geophys. Res. Atmos., 118, 10,994-911,006.

——, 2015: Onset of circulation anomalies during stratospheric vortex weakening events: the role of planetary-scale waves. J. Climate, submitted.

McLandress, C., and T. G. Shepherd, 2009: Impact of Climate Change on Stratospheric Sudden Warmings as Simulated by the Canadian Middle Atmosphere Model. J. Climate, 22, 5449-5463.

Nakagawa, K. I., and K. Yamazaki, 2006: What kind of stratospheric sudden warming propagates to the troposphere? Geophys. Res. Lett., 33, L04801.

Palmeiro, F. M., D. Barriopedro, R. Garcia-Herrera, and N. Calvo, 2015: Comparing Sudden Stratospheric Warming Definitions in Reanalysis Data. J. Climate, in press.

Polvani, L. M., and D. W. Waugh, 2004: Upward wave activity flux as a precursor to extreme stratospheric events and subsequent anomalous surface weather regimes. J. Climate, 17, 3,548-543,554.

Quiroz, R. S., 1975: The Stratospheric Evolution of Sudden Warmings in 1969–74 Determined from Measured infrared Radiation Fields. J. Atmos. Sci., 32, 211-224.

Uppala, S. M., and Coauthors, 2005: The ERA-40 re-analysis. Quart. Jour. Royal. Met. Soc., 612, 2961-3012.

Tables

Table 1 CMIP5 models used in this study and their classification.

Table 2 Sudden stratospheric warming (SSW) identified from the wind reversal and wind tendency definitions.

Figures

Fig. 1 Zonal-mean zonal winds (m s^{-1}) at 10 hPa and 60°N for (a) ERA40 and (b) CanESM2 models. The thin line across the x-axis denotes the 0 m s^{-1} threshold.

Fig. 2 Time series of major midwinter sudden stratospheric warming (SSW) events as defined using the wind reversal definition (left) and the wind tendency definition (right).

Fig. 3 (top left) Latitude and height cross-section of the climatological zonal-mean zonal winds ([u]; m s^{-1}) averaged from December to February (DJF) in ERA40. The contour interval is 10 m s^{-1}, and the zero line is indicated with a thick black line. (center and right) Same as the top left panel but for interannual variability of the DJF-mean [u] (center) and daily variability of [u] in DJF (right). For the daily variability, the mean value for each winter was subtracted from daily anomalies to remove the impact of the interannual variability. (middle and bottom rows) Same as the top row but for high-top (middle) and low-top (bottom) models. Statistically insignificant (t-test; $p > 0.05$) values are hatched, and difference from ERA40 (model-ERA40) is shown by shading.

Fig. 4 Scatter plot of the zonal-mean zonal wind climatology at 10 hPa and at 60°N and its daily standard deviation from CMIP5 models. Red, green, blue, and black colors indicate high-top, mid-top, and low-top models and ERA40 reanalysis, respectively. Solid lines range ±1 standard deviation among models while centered on their multi-model mean.

Fig. 5 Sudden stratospheric warming (SSW) frequency derived from (a) the wind reversal definition and (b) the wind tendency definition. Low-top, mid-top, and high-top models are colored blue, green, and red, respectively. The SSW frequency in ERA40 is indicated by the black horizontal line. Multi-model mean frequency and intermodel spread (1 standard deviation) are shown at the right of each panel.

Fig. 6 (a) Sudden stratospheric warming (SSW) frequency as a function of the threshold value of the zonal-mean zonal wind tendency at 10 hPa and 60°N and the evaluated time window for ERA40. (b) Difference between the high-top and low-top models. Difference between ERA40 and (c) high-top and (d) low-top models. Values statistically insignificant at the 95% confidence level are hatched. The two low-top models were ignored because their SSW events are extremely rare. The SSW frequency of six to eight events per decade from ERA40 is shown by with thick black lines in each panel. The numbers at the upper right corner in each panel indicates SSW frequency or its difference from ERA40 when the -1.1 m s^{-1} day^{-1} threshold and 30-day time window are used.

Fig. 7 (Top) Scatter plot of climatological zonal-mean zonal wind at 10 hPa and 60°N and sudden stratospheric warming (SSW) frequency for the wind reversal definition (left) and the wind tendency definition (right). (Bottom) Same as top panels but for eddy heat flux at 100 hPa integrated over 45–75°N. Low-top, mid-top, and high-top models are colored blue, green, and red, respectively. Black-dotted lines indicate the reference values in ERA40. The numbers shown in each panel denote the correlation coefficients for all (black), high-top (red), and low-top (blue) models. Statistically significant correlation coefficient at the 95% confidence level is indicated by the asterisk.

Fig. 8 Same as Fig. 4 but for sudden stratospheric warming (SSW) frequency introduced using the wind reversal definition (left) and the wind tendency definition (right). The circle size indicates the SSW frequency.

Fig. 9 Multi-model mean time series of zonal-mean eddy heat flux at 100 hPa integrated over 45–75°N during sudden stratospheric warming (SSW) detected by the wind reversal definition (left) and the wind tendency definition (right). Lag zero indicates the onset of SSW. Low-top and high-top models are denoted by blue and red colors, respectively. The reference time series, derived from ERA40, is shown in black.

Fig. 10 Time-height development of the northern annular mode (NAM) index during sudden stratospheric warming (SSW) events, as detected by the wind reversal definition (left) and the wind tendency definition (right) for ERA40 (top), high-top (middle), and low-top (bottom) models. The NAM index is based on polar-cap averaged geopotential height (>60°N). Shading interval of 1.0 is indicated by a white line. Hatching shows insignificant values (95%) when the multi-model spread is considered.

Fig. 11 (Top) Same as Fig. 5 but for RCP8.5 runs. (Bottom) Difference in sudden stratospheric warming (SSW) frequency between RCP8.5 and historical runs.

Table 1 CMIP5 models used in this study and their classification.

Model Name	Center	Vertical Level	Model Top	Classification
ACCESS1-0	ACCESS	38	39 km	Low
ACCESS1-3	ACCESS	38	39 km	Low
BCC-CSM1-1	BCC	26	2.917 hPa	Low
BCC-CSM1-1-M	BCC	26	2.917 hPa	Low
BNU-ESM	GCESS/BNU	26	2.194 hPa	Low
CanESM2	CCC	35	0.5 hPa	Mid
CCSM4	NCAR	27	2.194 hPa	Low
CMCC-CESM	CMCC	39	0.01 hPa	High
CMCC-CM	CMCC	31	10 hPa	Low
CMCC-CMS	CMCC	95	0.01 hPa	High
CNRM-CM5	CNRM	31	10 hPa	Low
CSIRO-Mk3-6-0	CSIRO/QCCCE	18	4.5 hPa	Low
FGOALS-g2	LASG/IAP	26	2.194 hPa	Low
GFDL-CM3	GFDL	48	0.01 hPa	High
GFDL-ESM2G	GFDL	24	3 hPa	Low
GFDL-ESM2M	GFDL	24	3 hPa	Low
HadGEM2-CC	MOHC	60	84 km	High
INMCM4	INM	21	10 hPa	Low
IPSL-CM5A-LR	IPSL	39	0.04 hPa	High
IPSL-CM5A-MR	IPSL	39	0.04 hPa	High
IPSL-CM5B-LR	IPSL	39	0.04 hPa	High
MIROC5	MIROC	40	3 hPa	Low
MIROC-ESM	MIROC	80	0.0036 hPa	High
MIROC-ESM-CHEM	MIROC	80	0.0036 hPa	High
MPI-ESM-LR	MPI	47	0.01 hPa	High
MPI-ESM-MR	MPI	95	0.01 hPa	High
MRI-CGCM3	MRI	48	0.01 hPa	High
NorESM1-M	NCC	26	3.54 hPa	Low

Table 2 Sudden stratospheric warming (SSW) identified from the wind reversal and wind tendency definitions.

Number	Central dates	
	WMO	tendency
1	31 Jan 1958	30 Jan 1958
2	17 Jan 1960	18 Jan 1960
3	28 Jan 1963	27 Jan 1963
4	16 Dec 1965	
5	23 Feb 1966	27 Feb 1966
6	7 Jan 1968	2 Jan 1968
7	28 Nov 1968	
8	13 Mar 1969	
9	2 Jan 1970	6 Jan 1970
10	18 Jan 1971	15 Jan 1971
11	20 Mar 1971	
12		28 Feb 1972
13	31 Jan 1973	1 Feb 1973
14		28 Feb 1974
15	9 Jan 1977	
16		2 Feb 1978
17		27 Jan 1979
18	22 Feb 1979	27 Feb 1979
19	1 Mar 1980	
20		31 Jan 1981
21	4 Mar 1981	
22	4 Dec 1981	
23		31 Jan 1983
24	24 Feb 1984	19 Feb 1984
25	1 Jan 1984	
26		3 Jan 1985
27	23 Jan 1987	24 Jan 1987
28	8 Dec 1987	10 Dec 1987
29	14 Mar 1988	
30	21 Feb 1989	11 Feb 1989
31		15 Feb 1990
32		4 Feb 1991
33		16 Jan 1992
34		18 Feb 1993
35		27 Jan 1995
36	15 Dec 1998	19 Dec 1998
37	26 Feb 1999	28 Feb 1999
38	20 Mar 2000	
39	11 Feb 2001	9 Feb 2001
40	31 Dec 2001	2 Jan 2002

41	18 Feb 2002	

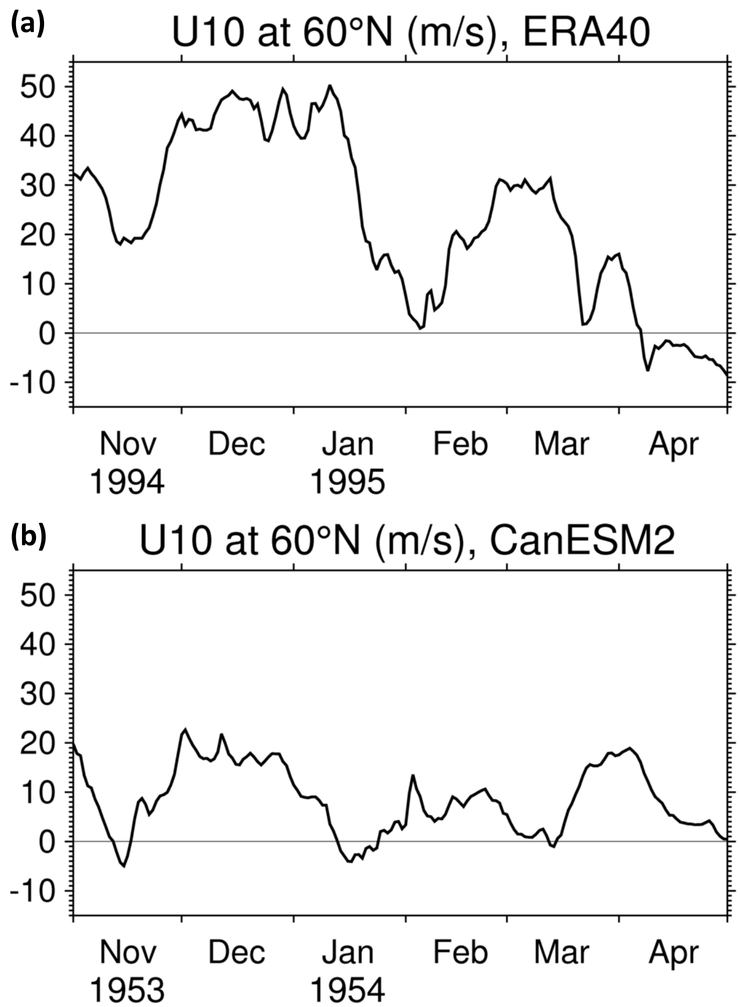

Fig. 1 Zonal-mean zonal winds (m s^{-1}) at 10 hPa and 60°N for (a) ERA40 and (b) CanESM2 models. The thin line across the x-axis denotes the 0 m s^{-1} threshold.

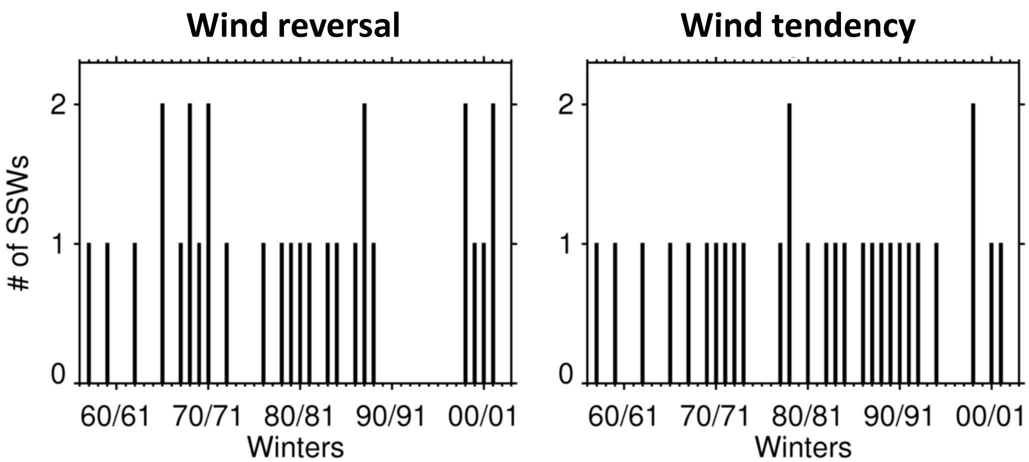

Fig. 2 Time series of major midwinter sudden stratospheric warming (SSW) events as defined using the wind reversal definition (left) and the wind tendency definition (right).

577

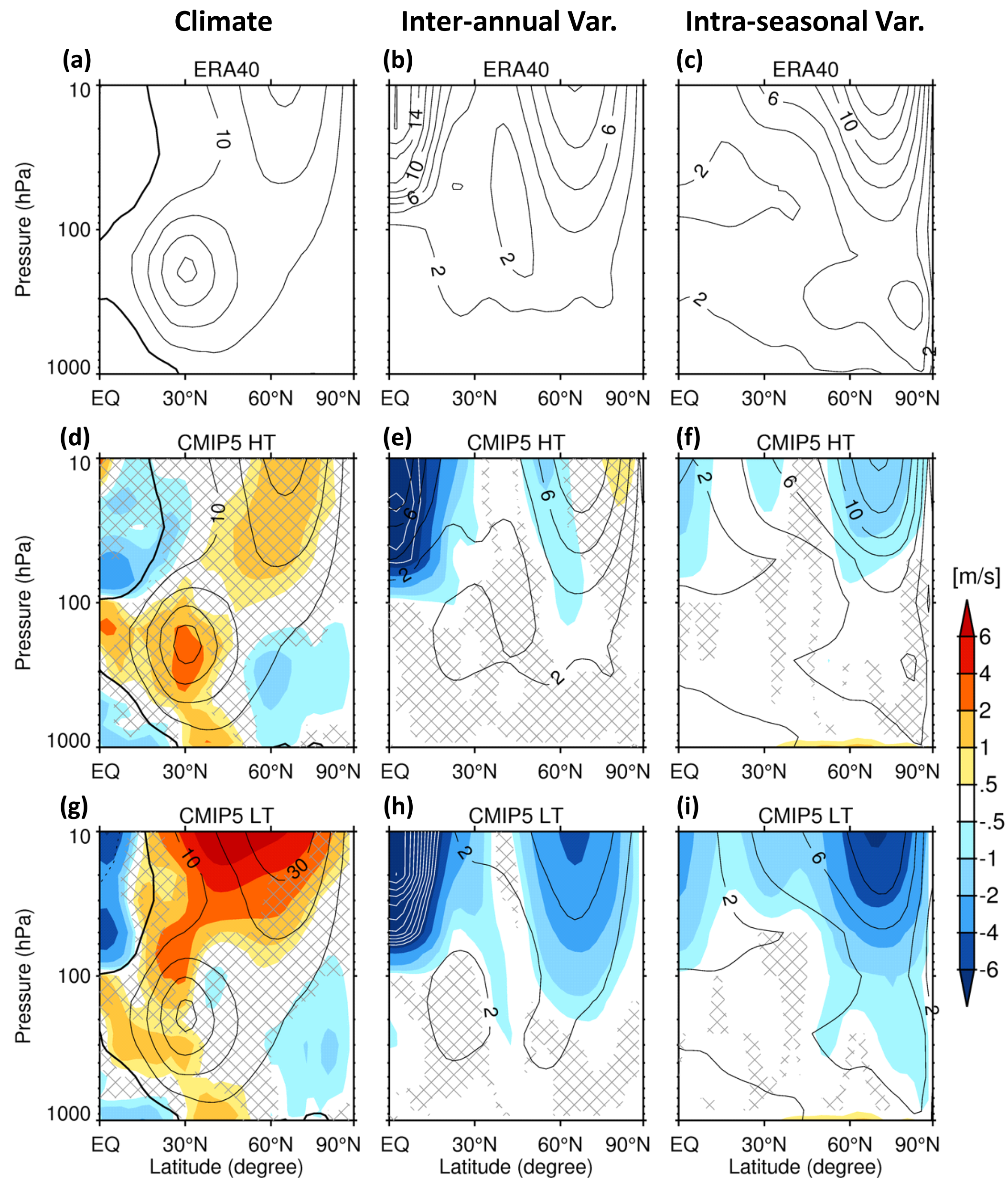

Fig. 3 (top left) Latitude and height cross-section of the climatological zonal-mean zonal winds ([u]; m s^{-1}) averaged from December to February (DJF) in ERA40. The contour interval is 10 m s^{-1}, and the zero line is indicated with a thick black line. (center and right) Same as the top left panel but for interannual variability of the DJF-mean [u] (center) and daily variability of [u] in DJF (right). For the daily variability, the mean value for each winter was subtracted from daily anomalies to remove the impact of the interannual variability. (middle and bottom rows) Same as the top row but for high-top (middle) and low-top (bottom) models. Statistically insignificant (t-test; $p > 0.05$) values are hatched, and difference from ERA40 (model-ERA40) is shown by shading.

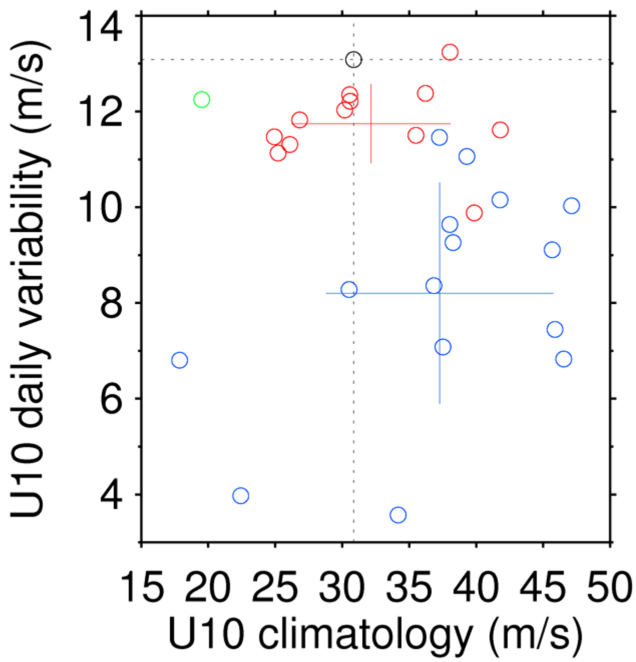

Fig. 4 Scatter plot of the zonal-mean zonal wind climatology at 10 hPa and at 60°N and its daily standard deviation from CMIP5 models. Red, green, blue, and black colors indicate high-top, mid-top, and low-top models and ERA40 reanalysis, respectively. Solid lines range ±1 standard deviation among models while centered on their multi-model mean.

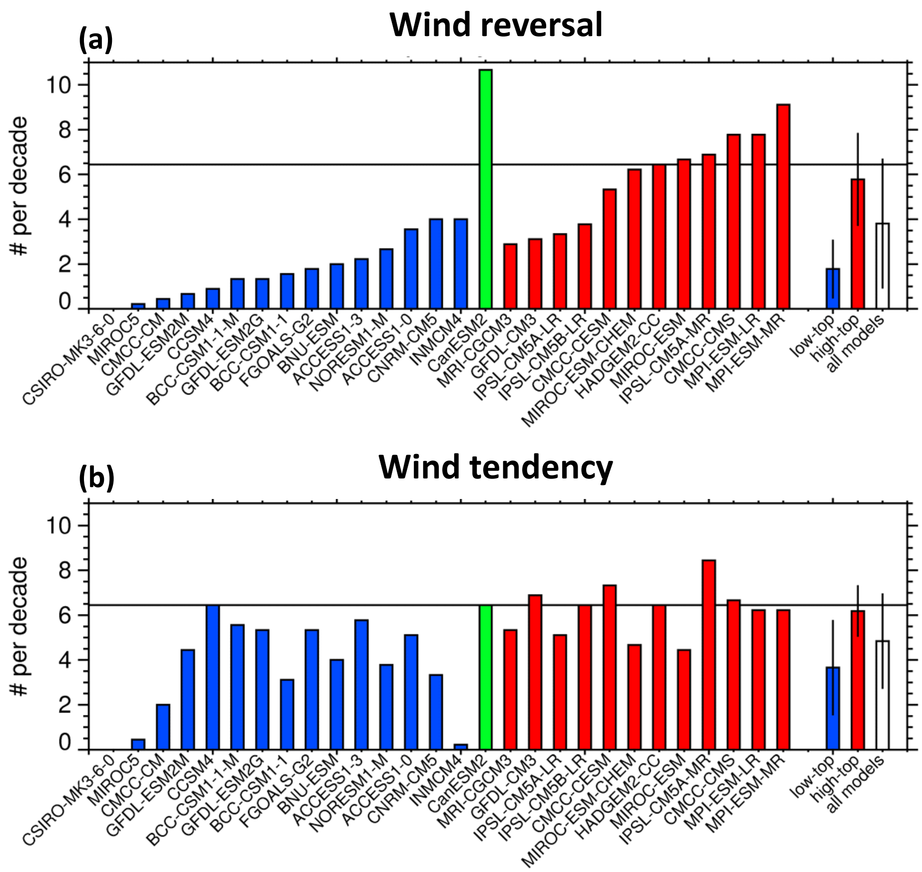

Fig. 5 Sudden stratospheric warming (SSW) frequency derived from (a) the wind reversal definition and (b) the wind tendency definition. Low-top, mid-top, and high-top models are colored blue, green, and red, respectively. The SSW frequency in ERA40 is indicated by the black horizontal line. Multi-model mean frequency and intermodel spread (1 standard deviation) are shown at the right of each panel.

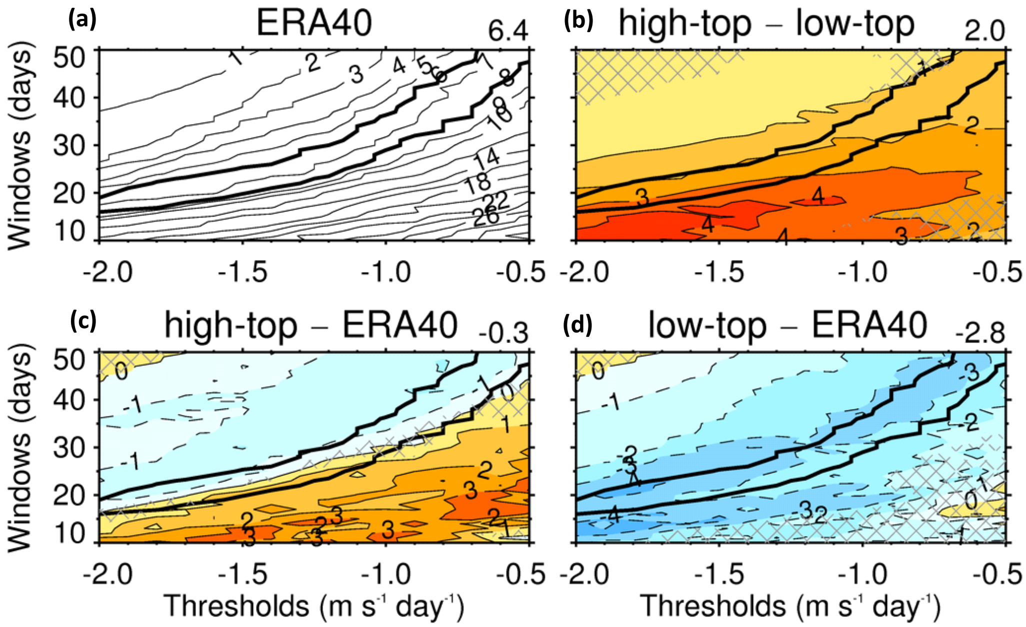

Fig. 6 (a) Sudden stratospheric warming (SSW) frequency as a function of the threshold value of the zonal-mean zonal wind tendency at 10 hPa and 60°N and the evaluated time window for ERA40. (b) Difference between the high-top and low-top models. Difference between ERA40 and (c) high-top and (d) low-top models. Values statistically insignificant at the 95% confidence level are hatched. The two low-top models were ignored because their SSW events are extremely rare. The SSW frequency of six to eight events per decade from ERA40 is shown by with thick black lines in each panel. The numbers at the upper right corner in each panel indicates SSW frequency or its difference from ERA40 when the -1.1 m s^{-1} day^{-1} threshold and 30-day time window are used.

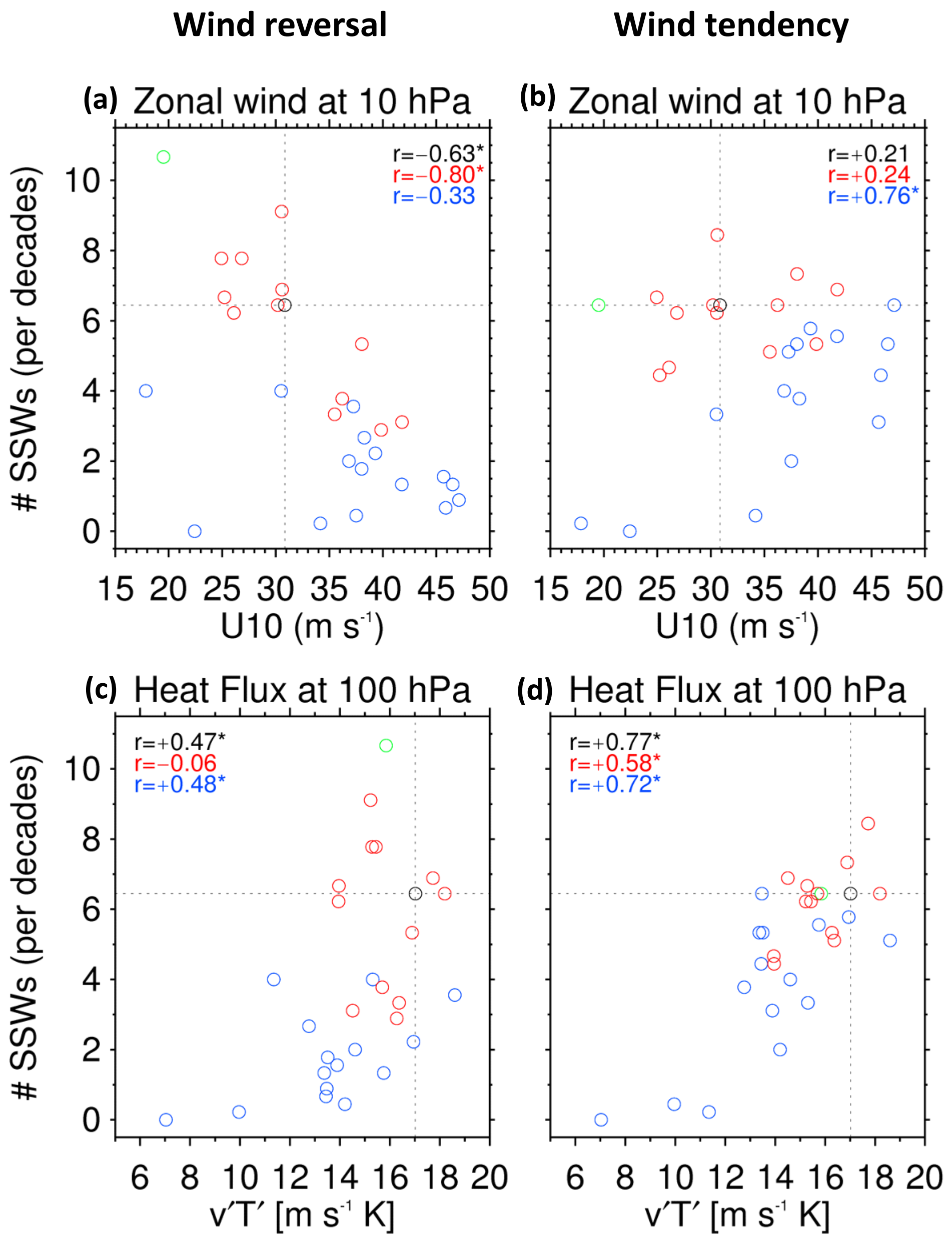

Fig. 7 (Top) Scatter plot of climatological zonal-mean zonal wind at 10 hPa and 60°N and sudden stratospheric warming (SSW) frequency for the wind reversal definition (left) and the wind tendency definition (right). (Bottom) Same as top panels but for eddy heat flux at 100 hPa integrated over 45–75°N. Low-top, mid-top, and high-top models are colored blue, green, and red, respectively. Black-dotted lines indicate the reference values in ERA40. The numbers shown in each panel denote the correlation coefficients for all (black), high-top (red), and low-top (blue) models. Statistically significant correlation coefficient at the 95% confidence level is indicated by the asterisk.

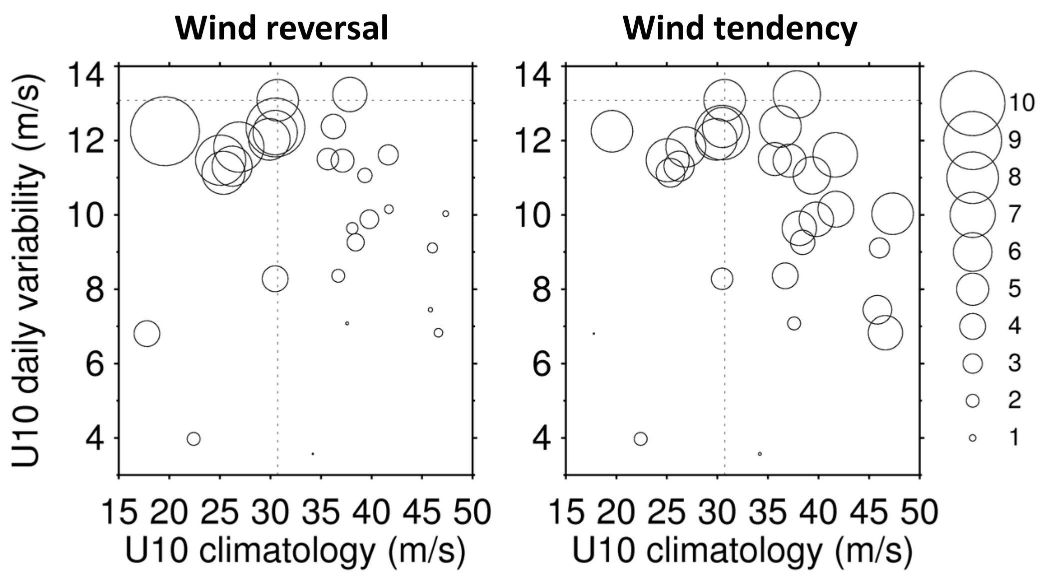

Fig. 8 Same as Fig. 4 but for sudden stratospheric warming (SSW) frequency introduced using the wind reversal definition (left) and the wind tendency definition (right). The circle size indicates the SSW frequency.

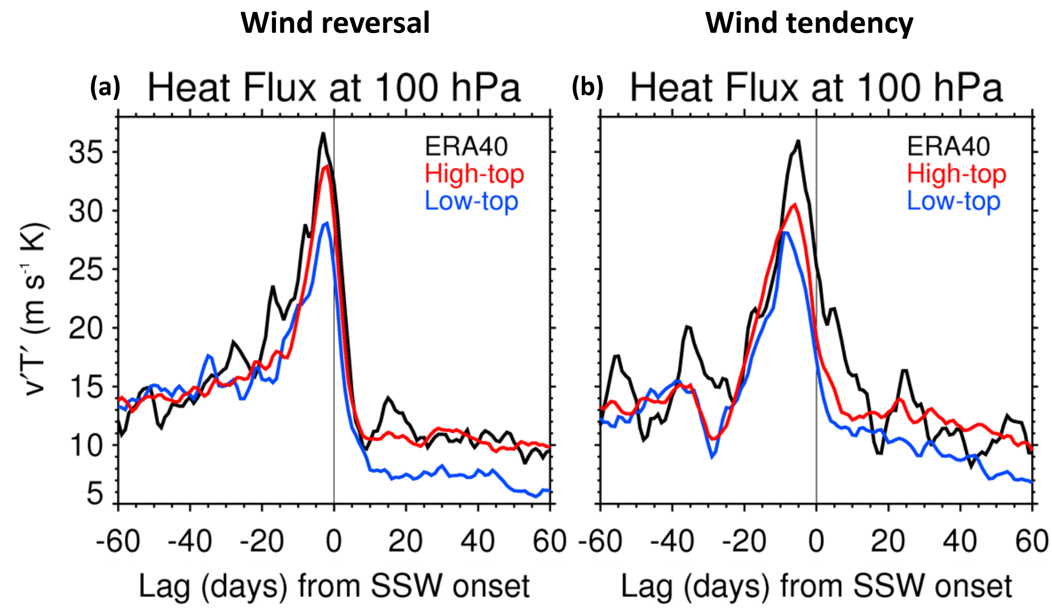

Fig. 9 Multi-model mean time series of zonal-mean eddy heat flux at 100 hPa integrated over 45–75°N during sudden stratospheric warming (SSW) detected by the wind reversal definition (left) and the wind tendency definition (right). Lag zero indicates the onset of SSW. Low-top and high-top models are denoted by blue and red colors, respectively. The reference time series, derived from ERA40, is shown in black.

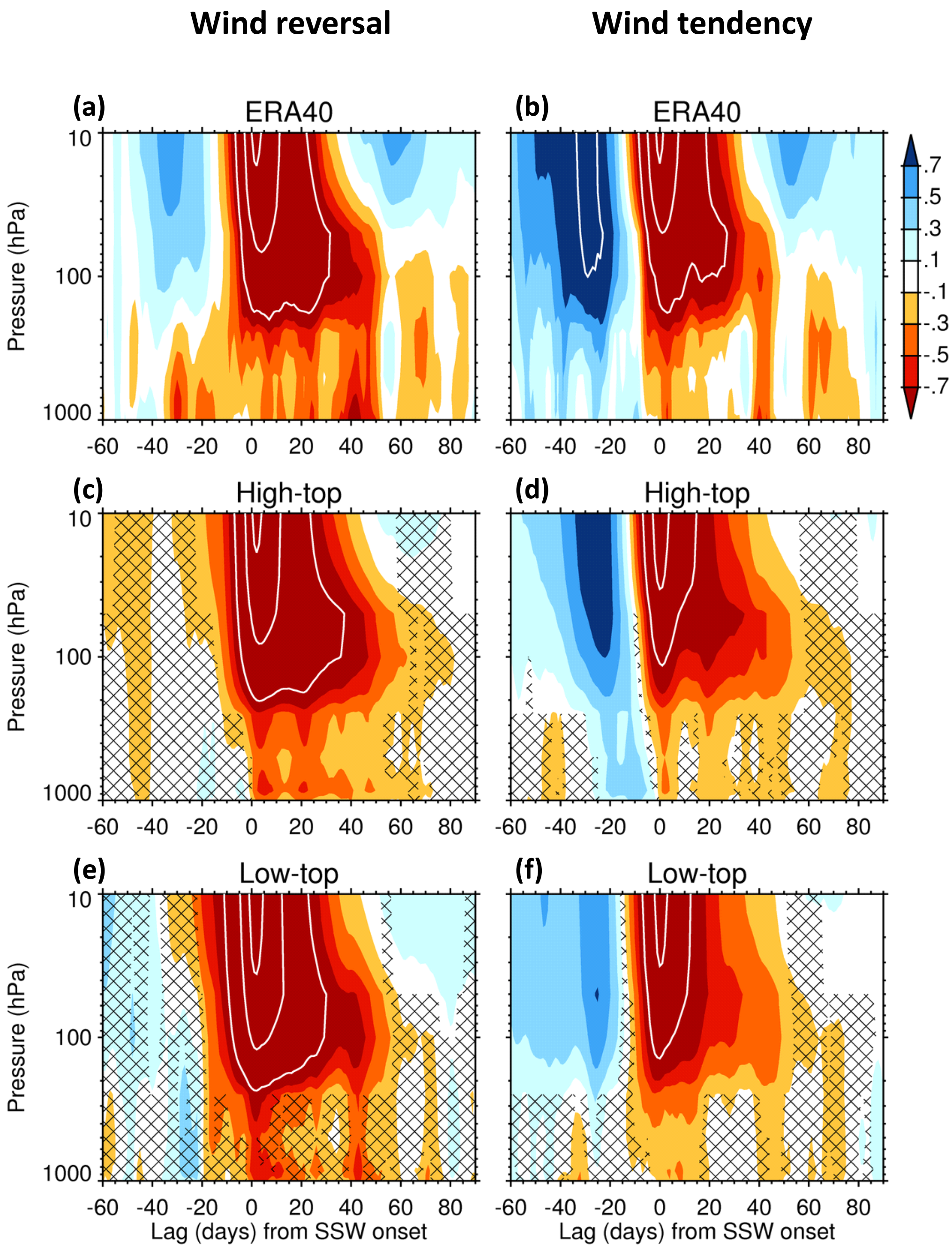

Fig. 10 Time-height development of the northern annular mode (NAM) index during sudden stratospheric warming (SSW) events, as detected by the wind reversal definition (left) and the wind tendency definition (right) for ERA40 (top), high-top (middle), and low-top (bottom) models. The NAM index is based on polar-cap averaged geopotential height (>60°N). Shading interval of 1.0 is indicated by a white line. Hatching shows insignificant values (95%) when the multi-model spread is considered.

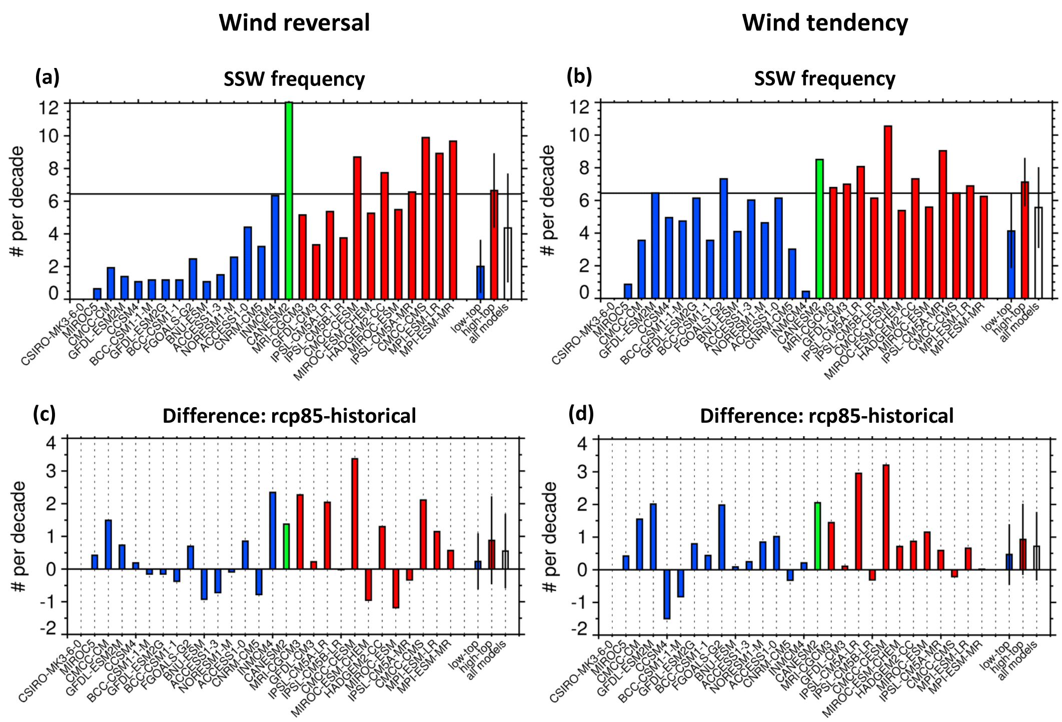

Fig. 11 (Top) Same as Fig. 5 but for RCP8.5 runs. (Bottom) Difference in sudden stratospheric warming (SSW) frequency between RCP8.5 and historical runs.